Figures and tables

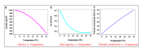
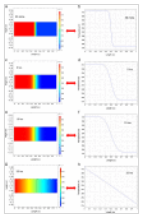
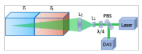
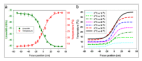
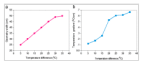
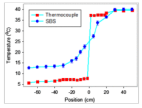
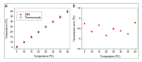

Optics Communications
Volume 363, 15 March 2016, Pages 21–25

Investigations on thermal-transfer characteristics of water based on stimulated Brillouin scattering

Jiulin Shi[a, b], , Hongpeng Wang[a, b], Jiacheng Qian[a, b], Xingdao He[a, b]
Show more

doi:10.1016/j.optcom.2015.11.003

Highlights

- An effective method for investigating the thermal-transfer of water was proposed.
- It is the first thermal-transfer measurements using the SBS method.
- The temperature profile can be described by measuring the linewidth of SBS spectrum.
- The more specific investigation on the thermocline is the subject of further studies.

Abstract

In this paper, we present a successful measurement of the thermal-transfer process of water in terms of stimulated Brillouin scattering (SBS) with a pulsed Nd:YAG laser as the light source. The temperature profiles between two different temperature layers can be determined through measuring the linewidth of SBS spectra. The measured results of thermal-transfer process of water are agree well with the theoretical simulation results based on the heat conduction equation. We have demonstrated that, the geometry width and temperature gradient of gradient layer depend on the temperature difference between T_1 and T_0 and different thermal-transfer times. This method presents an important step towards the practical application of a Brillouin lidar system, it could provide a potential technology for investigating the distribution characteristics of the thermocline in ocean.

Keywords

SBS; Line-width; Thermal-transfer; Thermocline

1. Introduction

The understanding of thermal conduction in liquids is a problem of great relevance in heat management applications, for instance, the dissipated heat of electronic devices can be efficiently transported through a liquid refrigerant recirculating system. The fundamental role that water plays in thermal management applications, since it presents the highest thermal conductivity observed in any molecular liquid. The thermal-transfer characteristics of water is also an important topic in hydrodynamic and biochemical processes, and have been subject to extensive theoretical and experimental investigations during the past decades [1], [2], [3] and [4]. Theoretically, the thermal conductivity of water can be computed by define suitable boundary conditions, for example, it is possible to estimate the thermal conductivity of water using the Green Kubo approach or by computing the fluid response to a distinct temperature gradient [5], [6],

[7] and [8]. Most studies have focused on a specific temperature and density or a narrow range of thermodynamic states [9], [10] and [11]. However, experimental studies on certain basic properties of thermal-transfer in water are still scanty, and some important characters during thermal-transfer process, such as geometrical width and temperature gradient at different time were seldom reported. In the present work, a new method for investigating the thermal-transfer characteristics of water based on stimulated Brillouin scattering [12], [13], [14], [15] and [16] at different temperature is proposed. Also, the temperature distribution between two different temperature layers is numerical simulated. Sequentially, distribution features of water temperature at different temperature differences are investigated experimentally and analyzed through analyzing the temperature dependence of the linewidth of SBS in water. The whole work is described as follows.

2. Theoretical consideration

In this work, the thermal-transfer process of water was considered based on the heat conduction equation:

$$\rho C_P \frac{\partial T}{\partial t} + \rho C_P u \cdot \Delta T = \nabla \cdot (\lambda \Delta T) + Q \quad (1)$$

Turn on

where, $C_P/C_V=1$, ρ is the density of water, C_P is the thermo capacity at constant pressure, T is the thermodynamic temperature of water, u is the speed in the direction of ΔT, λ is the thermal conductivity of water and Q is the heat resource. For the general case in terms of experimental conditions, we have $u=0$, $Q=0$. Then, the heat conduction equation can be simplified to the following expression:

$$\rho C_P \frac{\partial T}{\partial t} = \nabla \cdot (\lambda \Delta T) \quad (2)$$

Here, the temperature of water was varied from 5 °C to 40 °C in the natural environment. The thermal conductivity λ, the thermo capacity at constant pressure C_P, and the density ρ of water are the function of temperature T, and can be expressed respectively using:

$$\lambda = 0.561 + 0.002 \times T - (9.62 \times 10^{-6}) \times T^2 \quad (3)$$

$$C_P = 75.98 - 0.061 \times T + 0.002 \times T^2 - (1.755 \times 10^{-5}) \times T^3 \quad (4)$$

$$\rho = 999.86 + 0.058 \times T - 0.008 \times T^2 + (3.97 \times 10^{-5}) \times T^3 \quad (5)$$

Fig. 1 shows the changes of density, thermo capacity at constant pressure and thermal conductivity of water with the change of temperature. It can be seen that, they are neither constants nor linear change with temperature variation.

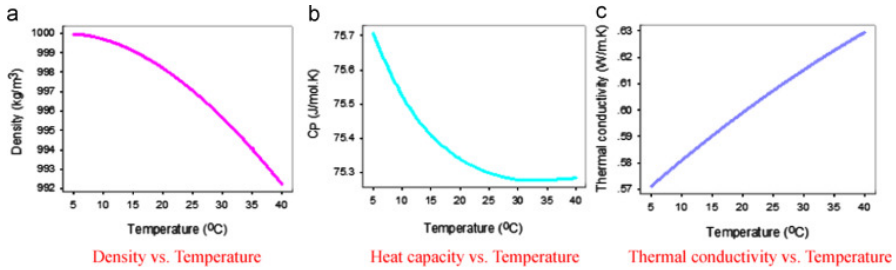

Fig. 1.
Changes of density, heat capacity, and thermal conductivity of water with the change of temperature.

Figure options

For simulating the thermal-transfer process, the first type boundary was chosen. Setting the lengths of the two layers are both 0.5 m, the temperature of the two layers are 5 °C and 40 °C, respectively:

$$T_0 = 40\ ^{\circ}\mathrm{C} (0 \le x \le 0.5\ \mathrm{m})$$

$T_1 = 5\ ^{\circ}\mathrm{C} (0.5 < x \leq 1\ \mathrm{m})$

Substituting the condition and (3), (4) and (5) into Eq. (2), the temperature distribution between the two layers can be numerical simulated, as shown in Fig. 2. The duration time for simulating the thermal-transfer process was 0–20 h, and Fig. 2 shows the simulated results at different time. One can see from the surface-temperature distribution that there is an obvious temporal variability of the thermal-transfer process of water, the thermal energy transferred gradually from high temperature layer (T_0) to low temperature layer (T_1). For comparison, the above evolution trait can also be observed from the line-temperature distribution. When the simulation time is 30 min, there is a remarkably thermocline between the high temperature layer and low temperature layer. With the increase of simulation time, the temperature distribution presents a gradient layer, and reaches steady state after 20 h and no stratification exists.

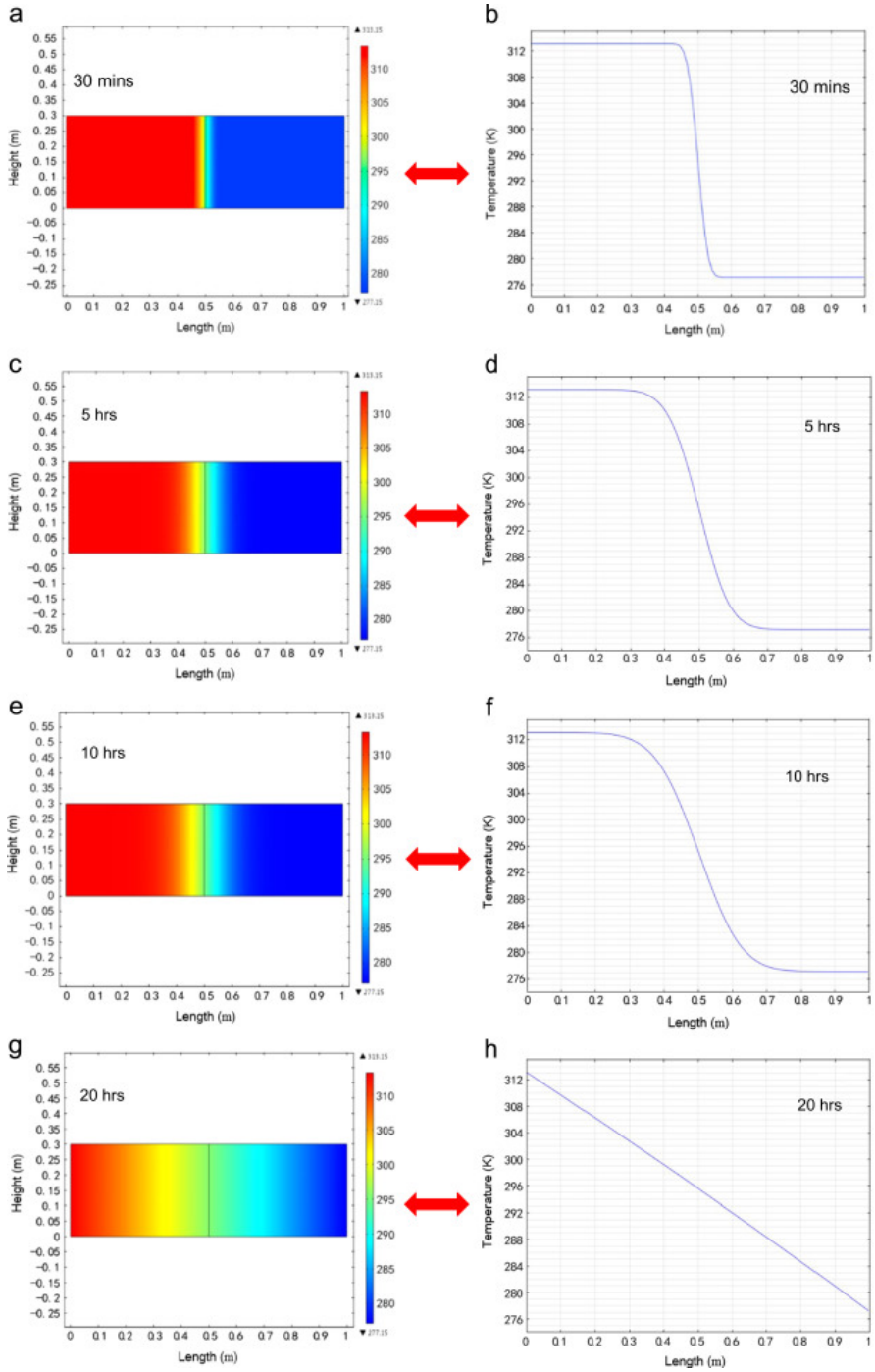

Fig. 2.
Simulated temperature distribution between the two layer with temperatures 40 °C and 5 °C at different

simulating time. (a), (c), (e), and (g) are the surface-temperature distribution, respectively; (b), (d), (f), and (h) are the corresponding line-temperature distribution, respectively.

Figure options

3. Experimental measurements and analysis

Basing on the theoretical simulations, we design the following experiments. The schematic diagram considered for experimental measurements is shown in Fig. 3. An injection-seeded, Q-switched and frequency-doubled Neodymium-doped Yttrium Aluminum Garnet (Nd:YAG) laser was used. The wavelength is ~532 nm, the pulse duration is ~8 ns, the repetition rate is 10 Hz. A narrow line-width (0.003 cm^{-1}) can be achieved by switching on the seeder. A thermostatic water tank with the size of 2 m length, 30 cm width and 30 cm high was made. A thin spectralite plate with the size of 1 mm thick, 30 cm width and 30 cm high was glued just at the center of the water tank, so the water tank was divided for two parts with the length of 1 m respectively. Each part was filled up the distilled water. It should be stated that between the two parts there is no water exchange and only the heat exchange exists. In order to reduce the reflection influence from the optical surfaces of the water tank, the normal direction of the front, the middle and the rear surfaces of the water tank was slightly deviated from the direction of the pump laser beam with an angle of ~5°.

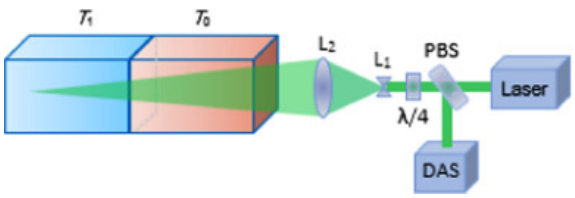

Fig. 3.
Setup configuration for experimental measurements. T_0 and T_1 represents the high and low temperature layer respectively, L_1 and L_2 are lenses, $\lambda/4$ is quarter-wave plate, PBS is polarization beam splitter, and DAS is data acquisition system.

Figure options

The polarization of the pump laser is horizontal, and becomes a circularly polarization along the 45° direction after passing through the polarization beam splitter (PBS) and quarter-wave plate. The laser beam was firstly diverged by a concave lens, then was focused by a converge lens with the focus length of 900 mm. The water tank was place on a translation stage, it can be moved alone with its length direction so that the focus point of the laser just hits on the point close to the dividing glass at the center of the water tank. The water temperature in the part of T_1 was set at 5 °C, while the water temperature in the part of T_0 was set from 10 to 40 °C. When the water temperature in the both parts were stable (after about 30 min), the laser was switched on, and the stimulated Brillouin scattering (SBS) can be excited at the focus point. The data acquisition system consisting of collimating lens, F-P etalon, and ICCD camera. Through measuring the linewidth of SBS the water temperature can be simply determined based on the following empirical equation [14] and [15]:

$$T=186.65\exp(-3.98\Gamma_B) \quad (6)$$

Here, Γ_B represents the measured linewidth of SBS.

Fig. 4 shows the distribution of water temperature and linewidth of SBS using the SBS method, here “0 cm” in horizontal axis represents the position of spectralite plate. Fig. 4(a) shows the measured linewidth of SBS and corresponding temperature of water at different focus position. For each data point, 30 spectrums of SBS were recorded, and mean values of the linewidth of SBS and water temperature are presented with error bars. In order to show more visually the relationship between the temperature distribution and the water temperature of part T_1 and T_0, Fig. 4(b) gives the temperature distribution in water tank when the temperature of part T_1 was set at 5 °C and part T_0 varied from

10 °C to 40 °C with the step of 5 °C. It can be seen that, the larger of the temperature difference between T_1 and T_0 is, the more obvious of the gradient layer in the middle position of water tank is. The measured results shown in Fig. 4 agree with the theoretical simulation results in Fig. 2.

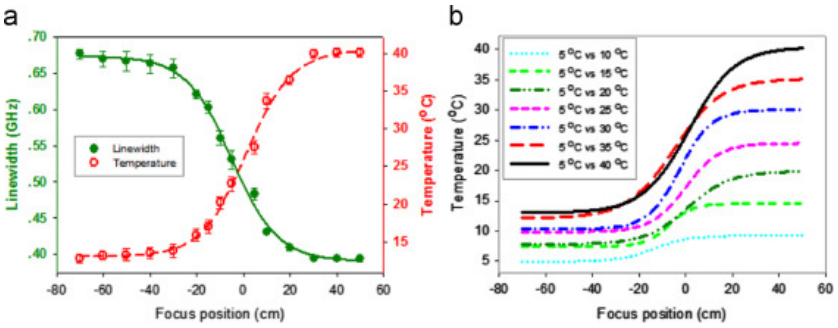

Fig. 4.
Experimental results using the SBS method. (a) Distributions of temperature and linewidth of SBS at the temperature of 5 °C (part T_1) and 40 °C (part T_0); (b) temperature distribution of water when the water temperature of part T_1 was set at 5 °C and part T_0 changed from 10 to 40 °C, respectively.

Figure options

For the purpose of expressing the thermal-transfer characteristics, two parameters that geometry width and temperature gradient are used in here. Geometry width denotes the width of gradient layer between T_1 and T_0, it corresponding to the changes of ≥10% of the temperature at the both layers, and the unit is “cm”. Temperature gradient denotes the temperature change per centimeter inside the range of the temperature width, and its unit is “°C/cm”. Fig. 5 shows the features of geometry width and temperature gradient at different temperature differences (the temperature of T_1 was set at 5 °C and T_0 varied from 10 °C to 40 °C with the step of 5 °C). These results indicate that: (i) the geometry width of gradient layer increases with the increase of temperature difference between two layers, and the maximum geometry width is about 50 cm and the minimum is only about 15 cm; (ii) the temperature gradient is proportional to the temperature difference between T_1 and T_0 layers.

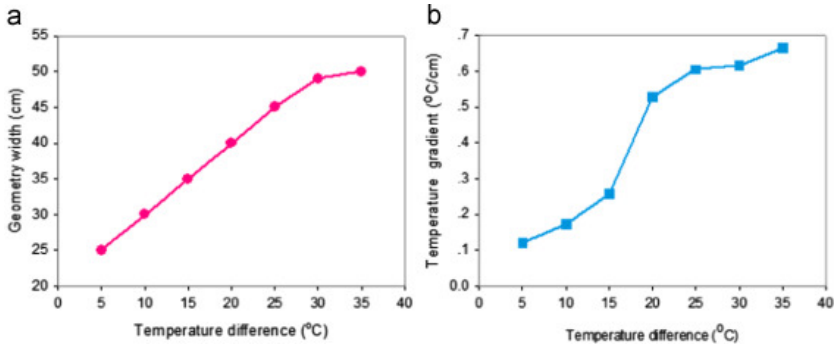

Fig. 5.
Distribution features of water temperature at different temperature differences in the parts T_0 and T_1 of the tank. (a) Geometry width; (b) temperature gradient.

Figure options

The thermal conductivities of water and optical glass around room temperature is about 0.66 W/m·K and 0.8 W/m·K, respectively. Because of the glass used is just 1 mm thick, its influence on the thermo flow could be neglected. In order to verify the feasibility of SBS method, we have conducted another following measurement using an electronic thermometer with the resolution of 0.01 °C. In this experiment, a high-density polythene (HDP) plate (thermal conductivity is 0.53 W/m·K) with 1 mm thick was used to replace the optical glass. Certain copper powders were mixed homogeneously into HDP so that the thermal conductivity of HDP can reach the value of 0.66 W/m·K. Then, the water

temperature was measured by employing the electronic thermometer (thermocouple), and the measured result is shown in Fig. 6. We can see that the temperature change is clearly visible. The measured geometry width is about 50 cm, which is nearly equal with the measured result through the SBS method. The difference of temperature gradient between the two methods is due to the pulse duration and focal length of laser beam. The more specific investigation on the spatial resolution in a long thermal-transfer system should be the subject of further studies.

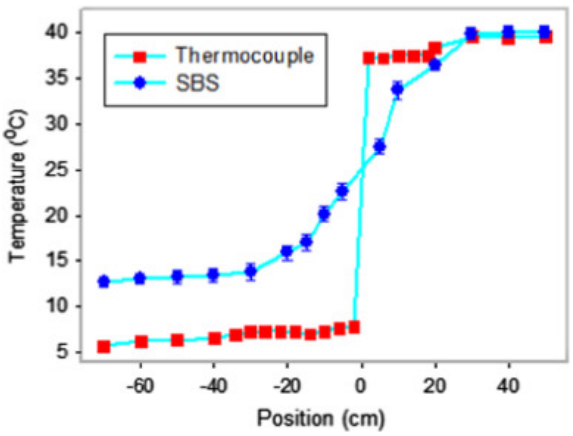

Fig. 6.
Measured temperature distribution using two different methods.

Figure options

Finally, in order to further show the feasibility of the SBS method, we give a simply assessment for the measured temperature difference between SBS method and thermocouple method at different water temperature, as shown in Fig. 7. Fig. 7(a) shows the measured results using the two different methods at the range of 5–40 °C, and Fig. 7(b) shows the temperature error of SBS method versus the measured value using a thermocouple. The maximum temperature error is about 0.36 °C.

Fig. 7.
Comparison of the measured temperature using SBS method with a thermocouple method.

Figure options

4. Conclusion and outlook

In conclusion, we have reported an effective method for investigating the thermal-transfer characteristics of water. To our knowledge these are the first thermal-transfer measurements using the SBS method. The temperature profiles between two different temperature layers can be recorded by measuring the linewidth of SBS spectrum. The theoretical and experimental results demonstrate the general feasibility of SBS method. The more specific investigation on the spatial resolution in a long thermal-transfer system should be the subject of further studies.

Acknowledgments

The authors gratefully acknowledge the National Natural Science Foundation of China (Grant nos. 41206084, 41576033, and 61465009) for financial support.

References

[1] H. Berendsen, J. Grigera, T. Straatsma
The missing term in effective pair potentials
J. Phys. Chem., 91 (1987), pp. 6269–6271

View Record in Scopus | Full Text via CrossRef | Citing articles (5514)

[2] C. Vega, J. Abascal
Simulating water with rigid non-polarizable models: a general perspective
Phys. Chem. Chem. Phys., 13 (2011), pp. 19663–19688

View Record in Scopus | Full Text via CrossRef | Citing articles (200)

[3] J.A. Whitehead
Thermohaline ocean processes and models
Annu. Rev. Fluid Mech., 27 (1995), pp. 89–113

View Record in Scopus | Full Text via CrossRef | Citing articles (32)

[4] Q. Zheng, X.H. Yan, J. Pan, V. Klemas
Nonlinear evolution of ocean internal solitons propagating along an inhomogeneous thermocline
J. Geophys. Res., 106 (2001), pp. 14083–14094

View Record in Scopus | Full Text via CrossRef | Citing articles (23)

[5] W.T. Ashurst, W.G. Hoover
Dense-fluid shear viscosity via nonequilibrium molecular dynamics
Phys. Rev. A, 11 (1975), pp. 658–678

View Record in Scopus | Full Text via CrossRef | Citing articles (288)

[6] B. Hafskjold, T. Ikeshoji, S.K. Ratkje
Molecular physics: an international journal at the interface between chemistry and physics
Mol. Phys., 80 (1993), pp. 1389–1412

View Record in Scopus | Full Text via CrossRef | Citing articles (126)

[7] A. Perronace, C. Leppla, F. Leroy, B. Rousseau, S. Wiegand
Soret and mass diffusion measurements and molecular dynamics simulations of n-pentane-n-decane mixtures
J. Chem. Phys., 116 (2002), pp. 3718–3729

View Record in Scopus | Full Text via CrossRef | Citing articles (71)

[8] N. Galamba, C.N. de Castro, J. Ely
Equilibrium and nonequilibrium molecular dynamics simulations of the thermal conductivity of molten alkali halides
J. Chem. Phys., 126 (2007), pp. 204511–204520

View Record in Scopus | Full Text via CrossRef

[9] M. Zhang, E. Lussetti, L. Souza, F. Müller-Plathe
Thermal conductivities of molecular liquids by reverse nonequilibrium molecular dynamics
J. Phys. Chem. B, 109 (2005), pp. 15060–15067

View Record in Scopus | Full Text via CrossRef | Citing articles (64)

[10] W. Evans, J. Fish, P. Keblinski
Thermal conductivity of ordered molecular water
J. Chem. Phys., 126 (2007), pp. 154504–154507

Full Text via CrossRef

[11] J. Muscatello, F. Römer, J. Sala, F. Bresme
Water under temperature gradients: polarization effects and microscopic mechanisms of heat transfer
Phys. Chem. Chem. Phys., 13 (2011), pp. 19970–19978

View Record in Scopus | Full Text via CrossRef | Citing articles (13)

[12] R.W. Boyd, K. Rzazewski, P. Narum
Noise initiation of stimulated Brillouin scattering
Phys. Rev. A, 42 (1990), pp. 5514–5521

View Record in Scopus | Full Text via CrossRef | Citing articles (253)

[13] J. Bai, J. Shi, M. Ouyang, X. Chen, W. Gong, H. Jing, J. Liu, D. Liu
Method for measuring threshold value of stimulated Brillouin scattering in water
Opt. Lett., 33 (2008), pp. 1539–1541

View Record in Scopus | Full Text via CrossRef | Citing articles (27)

[14] L. Zhang, D. Zhang, Z. Yang, J. Shi, D. Liu, W. Gong,and, E.S. Fry
Experimental investigation on linewidth compression of stimulated Brillouin scattering in water
Appl. Phys. Lett., 98 (3) (2011), p. 221106

View Record in Scopus | Full Text via CrossRef

[15] X. He, H. Wei, J. Shi, J. Liu, S. Li, W. Chen, X. Mo
Experimental measurement of bulk viscosity of water based on stimulated Brillouin scattering
Opt. Commun., 285 (2012), pp. 4120–4124

Article | PDF (566 K) | View Record in Scopus | Citing articles (3)

[16] J. Shi, Y. Tang, H. Wei, L. Zhang, D. Zhang, J. Shi, W. Gong, X. He, K. Yang, D. Liu
Temperature dependence of threshold and gain coefficient of stimulated Brillouin scattering in water
Appl. Phys. B, 108 (2012), pp. 717–720

View Record in Scopus | Full Text via CrossRef | Citing articles (9)

Corresponding author at: Jiangxi Engineering Laboratory for Optoelectronics Testing Technology, Nanchang Hangkong University, Nanchang 330063, China.